Front. Chem. Sci. Eng. 2022, 16(11): 1584−1594
https://doi.org/10.1007/s11705-022-2189-4

RESEARCH ARTICLE

Rare-earth separation based on the differences of ionic magnetic moment via quasi-liquid strategy

Na Wang[1,2], Fujian Li (✉)[2,3], Bangyu Fan[2,3,4], Suojiang Zhang[2,3], Lu Bai[2,3], Xiangping Zhang (✉)[2,3]

1 College of Chemical and Engineering, Zhengzhou University, Zhengzhou 450001, China
2 CAS Key Laboratory of Green Process and Engineering, State Key Laboratory of Multiphase Complex Systems, Beijing Key Laboratory of Ionic Liquids Clean Process, Institute of Process Engineering and Innovation Academy for Green Manufacture, Chinese Academy of Sciences, Beijing 100190, China
3 Ganjiang Innovation Academy, Chinese Academy of Sciences, Ganzhou 341000, China
4 College of Chemistry, Nanchang University, Nanchang 330031, China

Abstract The separation of rare earth elements is particularly difficult due to their similar physicochemical properties. Based on the tiny differences of ionic radius, solvent extraction has been developed as the "mass method" in industry with hundreds of stages, extremely intensive chemical consumption and large capital investments. The differences of the ionic magnetic moment among rare earths are greater than that of ionic radius. Herein, a novel method based on the large ionic magnetic moment differences of rare earth elements was proposed to promote the separation efficiency. Rare earths were firstly dissolved in the ionic liquid, then the ordering degree of them was improved with the Z-bond effect, and finally the magnetic moment differences between paramagnetic and diamagnetic rare earths in quasi-liquid system were enhanced. Taking the separation of Er/Y, Ho/Y and Er/Ho as examples, the results showed that Er(III) and Ho(III) containing ionic liquids had obvious magnetic response, while ionic liquids containing Y(III) had no response. The separation factors of Er/Y and Ho/Y were achieved at 9.0 and 28.82, respectively. Magnetic separation via quasi-liquid system strategy provides a possibility of the novel, green, and efficient method for rare earth separation.

Keywords rare earth element, different magnetic moment, magnetic separation, ionic liquid

1 Introduction

Rare earth elements (REEs) are composed of 17 elements including Lanthanide (La-Lu) and Scandium (Sc) & Yttrium (Y) in the element periodic table [1]. With unique characteristics of abundant 4f electrons and the large atomic magnetic moment of transition energy level, REEs are widely used in permanent magnet, luminescence, catalytic, and many other functional materials [2,3]. However, it is particularly difficult to separate and purify these elements due to the similar physicochemical properties [4,5]. With the increasing demand of high purity rare earth used in high-tech materials, innovative and efficient REEs separation and purification technology are highly desired.

To separate rare earth metals, fractional crystallization, ion exchange, solvent extraction, resin extraction, supercritical CO_2 extraction and membrane technology have been developed in recent years [6–12]. However, these methods are exploited based on the tiny differences in ionic radius among REEs, which determines the small separation factors. To conquer this drawback and promote the separation efficiency, the innovation of fundamental separation mechanism for efficient REEs separation is a radical approach.

The ionic magnetic moment and ionic radius have the similar intrinsic properties, generating from the movement of single electrons inside the atoms [13]. As known to all, the REEs separation factors (β) of solvent extraction, a mature industrial technology, are extremely small because of the slight differences among ionic radii. For example, $\beta_{Er/Y}$ is only 1.4 while $\beta_{Ho/Y}$ is approximately 1.64 by the 2-ethylhexylphosphonic acid mono-(2-ethylhexyl) ester (P507) [14], with the relative radii differences of Er(III)/Y(III) and Ho(III)/Y(III) of 0.1% and 1.6%, respectively [15]. However, the ionic magnetic moments of Er(III)/Y(III) and Ho(III)/Y(III) differ by 100% [16]. The large differences can be utilized for designing the efficient REEs separation process. In

Received April 1, 2022; accepted May 15, 2022

E-mails: fjli19@ipe.ac.cn (Li F.), xpzhang@ipe.ac.cn (Zhang X.)

1958, scientists firstly tried to apply magnetic separation of rare earth ions in aqueous solution [17]. Unsuccessfully, the magnetic moment of a single rare earth ion was too small to overcome Brownian motion, failing to form a total moment of magnetic force in water solution [18]. In aqueous solutions of rare earth chloride or nitrate, as a system lacking ion clusters, the enrichment effect was poor due to the large Brownian motion of the solution. After demagnetization, the concentration of enriched paramagnetic ions immediately decreased and eventually returned to a uniform solution [19]. The direct separation of rare earth ions in aqueous solution by using an external magnetic field was unfeasible. On the other hand, many rare earth oxides have strong magnetic properties, possible to use the magnetic separation method to recycle REEs [20]. Pearse et al. [21] constructed a system to separate mixed rare earth oxides and carbonates taking advantage of the difference in magnetic susceptibility of rare earths. Under the action of gravity and magnetic force, solid rare earth oxides with high magnetic susceptibility would be preferentially separated and absorbed by a magnetic field. Although the magnetic susceptibility of REEs in the solid-state is high, the interaction between internal ions is extremely strong. Therefore, the magnetic separation efficiency is low as it only separates the solid particles with different magnetism but loses to act on the different REEs in the particles. It is imperative to develop a new system for efficient and green REEs separation.

As a new class of solvents, ionic liquids (ILs) have the advantages of a wide range of temperatures, low flammability, negligible volatility, easy design and magnetic adjustment, being considered as "green solvents" [22–24]. The advantages of the highly efficient, green and simple process have been widely recognized by researchers [25–27]. Moreover, paramagnetic metals can be dissolved in ILs, producing a certain degree of magnetization under the external magnetic field, which is called as magnetic ionic liquids. In 2004, Hayashi [28,29] firstly proposed and synthesized the paramagnetic [bmim][$FeCl_4$], claiming that it was completely different from the conventional magnetic fluids, and that its magnetic response was far greater than that of $FeCl_3$ aqueous solution. Similarly, the ILs containing paramagnetic rare earth ions have strong magnetic response. Due to the long-range nature of coulomb interactions, ILs have a higher degree of structural ordering than organic liquids. Zhang et al. [30,31] originally proposed a new concept of Z-bond in the atomic/molecular scale, which was formed by the strong coupling between the hydrogen bond and electrostatic attraction. The Z-bond in ILs coupling with solid structure can form the intermediate degree of ordering quasi-liquid (QL) system, which differs from the long-range order of a crystal and the short-range order of a liquid [32]. As a new sight of matter state, QL is in the intermediate state between solid and liquid in the aspect of structures, dynamics, and transport properties [33]. As we all know, the Brownian motion of ions in aqueous solution is too great to form magnetic interaction force, while the lattice force of solids (such as rare earth oxides) is too strong for magnetic interaction to overcome the lattice force to separate REEs placed in it [34]. Different from conventional liquids with the chaotic orientation and arrangement, QL systems can improve the order degree of basic units through precise regulation, which provide a possibility to regulate Brownian motion of ions while weakening lattice force, allowing for separation of paramagnetic/diamagnetic rare earth ions by means of external magnetic fields.

Based on the above analysis, ILs, as green solvents, can be used for the efficient dissolution and separation of REEs. In the work, a novel method based on the large ionic magnetic moment differences of rare earth ions (RE(III)) was proposed to promote the separation efficiency. REEs were firstly dissolved in the ILs to form the QL system. Under an external magnetic field, the order degree of RE(III) was improved with the Z-bond effect, which strengthened the magnetic moment differences between paramagnetic and diamagnetic RE(III) in the QL system. The separation of Er/Y, Ho/Y and Er/Ho was presented as an example and the results were showed that it was feasible to separate the paramagnetic and diamagnetic RE(III) in ILs under the external magnetic field. The separation factors between Er/Y and Ho/Y were improved significantly and the separation mechanism was investigated carefully. The study may provide potential for the industrial application of magnetic separation in the future.

2 Experimental

2.1 Reagents

Trinity (tetragonal) phosphine chloride (97% purity) and erbium chloride hexahedron (99.99% purity) were purchased from McLean. Yttrium and holmium chloride hexahedron (99.99% purity) were bought from Damas-beta. The aqueous solutions with concentration of 0.55 $mol \cdot L^{-1}$ were prepared by dissolving the corresponding amount of rare earth metal chloride salt in deionized water. Nitric acid and ethanol were purchased from Sino pharm Chemical Reagent Co., Ltd. None of the reagents were further purified, and the experimental water was redistilled from deionized water.

2.2 Preparation of ionic liquids

Paramagnetic/diamagnetic REEs ILs were synthesized based on paramagnetic/diamagnetic rare earth ions with large magnetic moment differences. The synthetic processes of ILs are briefly introduced below.

$[P_{666,14}]_3[ErCl_6]$: 0.03 mol $[P_{666,14}][Cl]$ and 0.01 mol $ErCl_3{\cdot}6H_2O$ were dissolved in ethanol and added to a round-bottomed flask. Then, magnetic stirring was performed at 303 K for 5 h. Besides, ethanol and tiny amounts of water were removed by a rotary evaporator at 353 K. Finally, the compounds were dried overnight in a vacuum at 358 K using P_2O_5 as a desiccating agent, to obtain the pale pink liquid $[P_{666,14}]_3[ErCl_6]$.

$[P_{666,14}]_3[YCl_6]$: 0.03 mol $[P_{666,14}][Cl]$ and 0.01 mol $YCl_3{\cdot}6H_2O$ were dissolved in ethanol and added to a round-bottomed flask. Then, magnetic stirring was performed at 303 K for 5 h. Then, ethanol and tiny amounts of water were removed by a rotary evaporator at 353 K. Finally, the compounds were dried overnight in a vacuum at 358 K using P_2O_5 as a desiccating agent, to gain the colorless transparent liquid $[P_{666,14}]_3[YCl_6]$.

$[P_{666,14}]_3[HoCl_6]$: 0.03 mol $[P_{666,14}][Cl]$ and 0.01 mol $HoCl_3{\cdot}6H_2O$ were dissolved in ethanol in a round-bottomed flask. Then, magnetic stirring was performed at 303 K for 5 h. Then, ethanol and tiny amounts of water were removed by a rotary evaporator at 353 K. Finally, the compounds were dried overnight in a vacuum at 358 K with the desiccating agent P_2O_5, to get the faint yellow liquid $[P_{666,14}]_3[HoCl_6]$. More details were provided in Figs. S1–S3 in Electronic Supplementary Material (ESM).

2.3 Apparatus and measurements

The concentrations of RE(III) in ILs were measured by ICPE-9000 (Shimadu, Japan), and the concentrations of RE(III) in the ILs phase were calculated by the mass balance method. The Raman spectroscopy of chloride rare earth solids, ILs and aqueous solutions were determined by Raman spectrometry (Invia, Britain), and its excitation wavelength was 532 nm. The strength of the magnetic field and the gradient of the field (B∇B) were measured with a portable digital Gauss meter (WT106) by moving the probe away from the central point of the magnetic surface in steps of 1 mm. The density of the ILs was measured using a viscosity/density meter (DMA5000M-Lovis2000ME, Austria). The magnetic properties of $ErCl_3{\cdot}6H_2O$(S), $[P_{666,14}]_3[ErCl_6]$ (QL) and $ErCl_3$ water solution(L) were analysed by the Quantum Design Company MPMS SQUID (MPMS-3, America) at the 298 K and 500 Oe magnetic field.

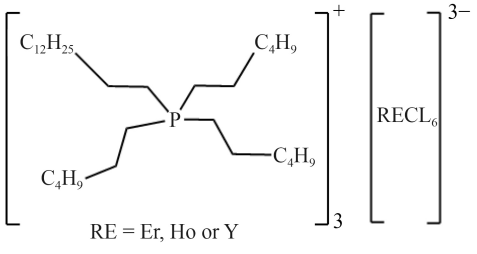

Fig. 1 Chemical structure of the three ILs.

2.4 Procedure

Stripping tests for metal in the mixed ILs system were performed with HNO_3, HCl solutions. Compared with HCl solution, the metal stripping efficiency with HNO_3 solution was better, with no degradation of the ionic liquid extraction phase [35]. Therefore, the concentration of REEs was determined as described below; the contents of rare earth metals Er(III), Ho(III) and Y(III) in ILs were separated by 4 $mol{\cdot}L^{-1}$ HNO_3 solution. The uniform standard for ILs phase sampling during the experiment was 0.1 mL. Stripping experiments of rare earth metals were conducted by using 0.1 mL ILs phase and 1.0 mL HNO_3 (4 $mol{\cdot}L^{-1}$) water solution. It was found that 1.0 mL nitric acid solution was in the lower layer and ILs phase containing rare earth metal was in the upper layer. The stripping process of rare earth metals is essentially the transfer of rare earth ions from the ILs phase to the water phase. In this system, the gravity of rare earth ions promoted their transfer, thus accelerating the mass transfer rate. In a constant temperature water bath oscillation chamber with the temperature set at 298 K and rotation speed set at 200 $r{\cdot}min^{-1}$, the contact reached equilibrium for 15 min, and the separation of the two phases was performed at 9000 $r{\cdot}min^{-1}$ for 4 min.

3 Results and discussion

3.1 Volumetric magnetic susceptibility of RE(III) compounds

To prove the hypothesis, the paramagnetic Er(III), Ho(III) and diamagnetic Y(III) were chosen as examples because the separation factors of Er(III)/Y(III) and Ho(III)/Y(III) were the smallest of all the series elements by P507 [14]. In order to confirm the magnetism of the different RE(III) states, the magnetic moment of Er(III) in the three states of $ErCl_3$ water solution(L), $[P_{666,14}]_3[ErCl_6]$(QL) and $ErCl_3{\cdot}6H_2O$(S) were firstly determined. The samples in different states were analysed as the same amount of 0.00055 mol, with the concentration of 0.55 $mol{\cdot}L^{-1}$ $ErCl_3$ water solution(L) and $[P_{666,14}]_3[ErCl_6]$(QL). The volumetric magnetic susceptibility of $HoCl_3{\cdot}6H_2O$(S), $[P_{666,14}]_3[HoCl_6]$(QL) and $HoCl_3$ water solution(L) were measured under the same way. All of the tests were sampled three times and the averaged results were obtained. As shown in Fig. 2, the volumetric magnetic susceptibility of rare earth chloride Er(III) with the same molar amount in the three states of $ErCl_3{\cdot}6H_2O$ crystal, $[P_{666,14}]_3[ErCl_6]$ and $ErCl_3$ in aqueous solution is 2.18, 2.03 and 1.84, respectively. They are different in the three states, although they have the same theoretical magnetic moment of Er(III) (9.58 μ_B). Obviously, the volumetric magnetic susceptibility of the three states lies as:

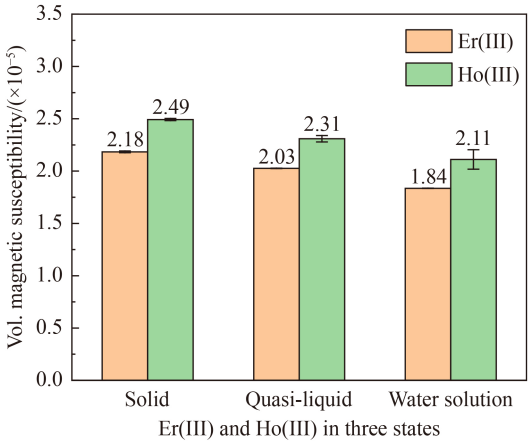

Fig. 2 Volumetric magnetic susceptibility of RE(III) compounds in the three states.

$ErCl_3 \cdot 6H_2O$(S) > $[P_{666,14}]_3[ErCl_6]$(QL) > $ErCl_3$ water solution(L). The states of paramagnetic atom have a great influence on its magnetic susceptibility.

On the other hand, the measured volumetric magnetic susceptibility of Ho(III) in the same state is greater than that of Er(III). It can be reasoned as the theoretical magnetic moment of Ho(III) (10.61 μ_B) is larger than Er(III) (9.58 μ_B). Generally, the greater the ionic magnetic moment is, the greater the susceptibility is [36]. As for lanthanide ions, the magnetic moment of Ho(III) is larger than Er(III) due to the more single electrons. To be concluded, the susceptibility of a certain compound is affected by two factors: the magnetic moment of the paramagnetic atom itself and the compound state.

3.2 The RE(III) ordering in the three states

To better explain this consequence, the internal molecular structure diagrams of $ErCl_3 \cdot 6H_2O$ crystal, $[P_{666,14}]_3[ErCl_6]$ and $ErCl_3$ in aqueous solution were proposed. As shown in Fig. 3, the anions and cations in the crystal molecular structure are closely arranged with a high degree of ordering, and the magnetic susceptibility is the maximum when the magnetic field is applied [37]. Then, as liquidized crystals, $[P_{666,14}]_3[ErCl_6]$ have a related ordered structure, but they are not exactly the same as the crystal structure. Therefore, interactions within crystal molecules are also effective in ILs [38–41]. Ordered clusters of molecules can be formed highly inside the QL system, the direction of the molecular cluster is consistent with the direction of the magnetic field when the magnetic field is applied. This explains why the magnetic susceptibility of the RE(III) in the QL system is close to that of the RE(III) solid. Finally, the ions in the water solution are disorderly arranged due to the large Brownian motion, and the force direction is all-directional. In the case of an external magnetic field, it is difficult for the magnetic moment to form an effective resultant force [19,42], so the volumetric magnetic susceptibility of RE(III) in water solutions is ignorable.

To sum up, the magnetic susceptibility is a macroscopic reflection of the resultant force of the magnetic moment inside the molecule and is closely related to the degree of ordering of molecules contained in substances. The root cause lies in the internal structure of the molecule and the interaction between anions and cations.

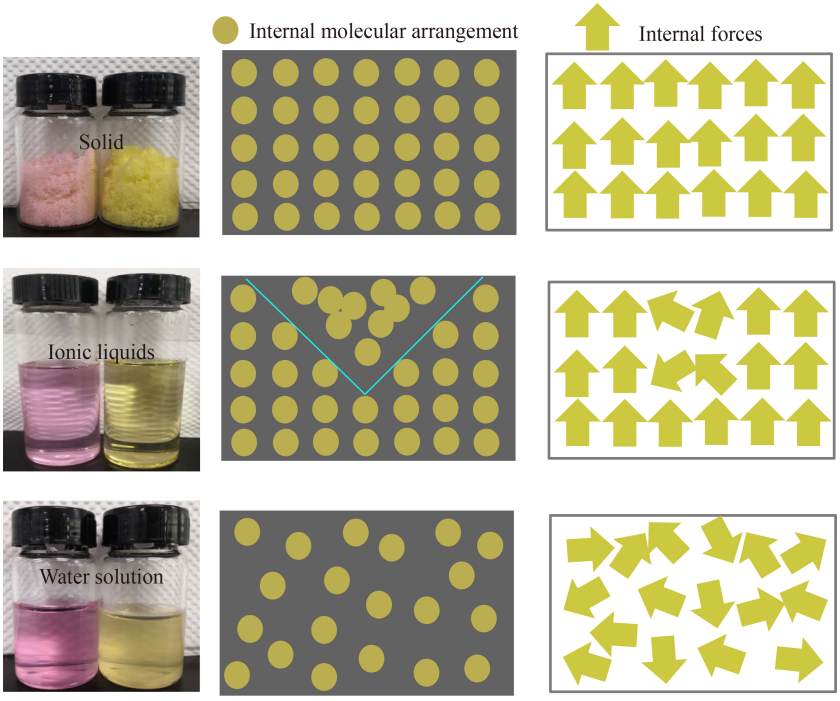

Fig. 3 Internal structure diagrams of the three states under the gradient magnetic field.

3.3 Raman spectroscopy of Er(III) compounds

To further verify the prediction of the ordering of paramagnetic rare earth ILs, the Raman spectroscopy of the three states were studied. The Raman spectroscopy of the $[bmim]^+$ cation in crystalline and liquid [bmim][X] highly resemble each other, indicating that their structures in IL state are similar to those in the crystalline state in the paper [40,41]. The structure information of $[P_{666,14}]_3[ErCl_6]$ and $[P_{666,14}][Cl]$, $ErCl_3{\cdot}6H_2O$ crystal and $ErCl_3$ in water solution is shown in Fig. 4. The Raman spectroscopy of ILs $[P_{666,14}]_3[ErCl_6]$ and $[P_{666,14}][Cl]$ agree well with each other. The $[P_{666,14}]^+$ in $[P_{666,14}]_3[ErCl_6]$ has a similar structure to that in $[P_{666,14}][Cl]$. That is because the Raman bands observed in $[P_{666,14}]_3[ErCl_6]$ and $[P_{666,14}][Cl]$ are all assigned to the vibrations of the $[P_{666,14}]^+$ cation. Notably, the Raman peaks of 776 and 552 cm^{-1}, which were characteristic peaks of the $ErCl_3$ crystal, were observed in $[P_{666,14}]_3[ErCl_6]$ and $ErCl_3{\cdot}6H_2O$ crystal, while they were absent in $[P_{666,14}][Cl]$ and $ErCl_3$ in water solution. It indicates that the similar ordered structure of $ErCl_3$ crystal is both in $[P_{666,14}]_3[ErCl_6]$ and $ErCl_3{\cdot}6H_2O$ crystal, but it cannot be observed when $ErCl_3$ is dissolved in water solution due to thermal motion. The peaks of water molecules (3200–3400 cm^{-1}) have also been claimed by the paper [43].

Combining the above conclusions with the measured volumetric magnetic susceptibility data, ILs, as the green solvents, can greatly enhance the order of internal molecules and have higher structural ordering than aqueous solutions.

3.4 Magnetic properties of RE(III) containing ionic liquids

Then, paramagnetic ILs (i.e., $[P_{666,14}]_3[ErCl_6]$ and $[P_{666,14}]_3[HoCl_6]$) and diamagnetic IL (i.e., $[P_{666,14}]_3[YCl_6]$) were synthesized respectively. In order to further verify whether the paramagnetic Er(III), Ho(III) and diamagnetic Y(III) in the QL system have changed, the magnetic properties of $[P_{666,14}]_3[ErCl_6]$, $[P_{666,14}]_3[HoCl_6]$ and $[P_{666,14}]_3[YCl_6]$ were examined by using the SQUID method. The magnetic moment of $[P_{666,14}]_3[ErCl_6]$ was measured at 300 K in the magnetic field range of −20000 to 20000 Oe using the MPMS SQUID measuring system. $[P_{666,14}]_3[HoCl_6]$ and $[P_{666,14}]_3[YCl_6]$ were also tested in the same condition. As indicated in Fig. 5, typical properties of paramagnetic Er(III)/Ho(III) and diamagnetic Y(III) were obtained. At the same time, the magnetic moment at 500 Oe in the temperature range of 10–300 K was measured (more details were provided in Fig. S4 in ESM). The variation of the magnetic moment values with the external magnetic field indicated that $[P_{666,14}]_3[ErCl_6]$ and $[P_{666,14}]_3[HoCl_6]$ were paramagnetic and the $[P_{666,14}]_3[YCl_6]$ was diamagnetic. No strong coupling among the spin angular momenta of the $[ErCl_6]^{3-}$ and $[HoCl_6]^{3-}$ anions was detected. Preliminary measurements of relationship between the magnetic moment and the temperature showed that the $[P_{666,14}]_3[ErCl_6]$ and $[P_{666,14}]_3[HoCl_6]$ exhibited ordinary paramagnetic temperature dependence in the temperature range 10 to 300 K; especially at lower temperature, the difference of magnetic moments increased obviously.

The influence of magnetic substance content on the magnetic size of the ionic liquid and the magneto-swimming velocity was studied. In the first place, the paramagnetic ionic liquid $[P_{666,14}]_3[ErCl_6]$ and diamagnetic ionic liquid $[P_{666,14}]_3[YCl_6]$ were mixed evenly according to a certain mole ratio, and mixed ILs 1–6 with different paramagnetic Er(III) contents were obtained. The specific proportion of mixing is shown in Table 1. Magnetic moment data were obtained by continuous testing at 298 K and 500 Oe using the MPMS SQUID magnetic measurement system. To avoid the deviation of the magnetic moment of the test results caused by the error of the massive size of the sample, quality magnetic susceptibility was obtained by further

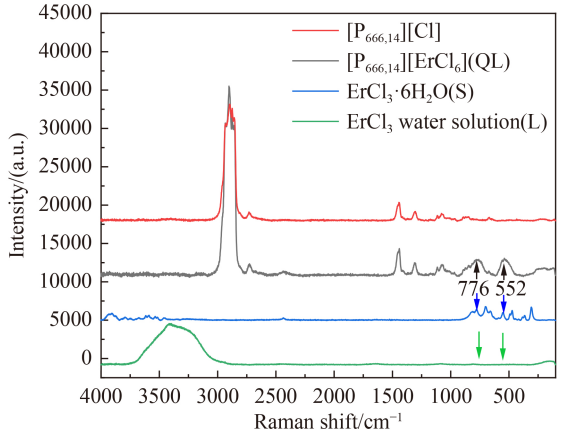

Fig. 4 Raman spectroscopy of $[P_{666,14}][Cl]$, $[P_{666,14}]_3[ErCl_6]$(QL), $ErCl_3{\cdot}6H_2O$(S) and $ErCl_3$ in water solution(L).

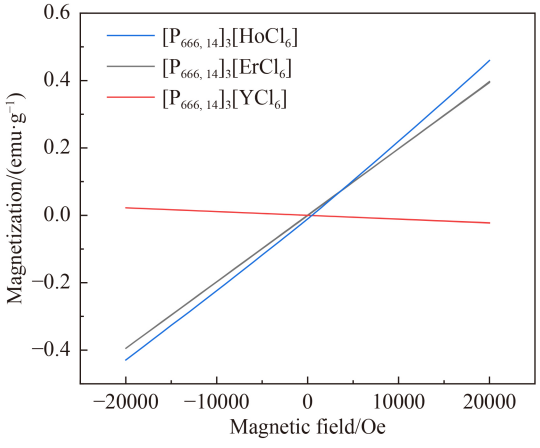

Fig. 5 Relationship between the magnetization and magnetic field of $[P_{666,14}]_3[ErCl_6]$, $[P_{666,14}]_3[HoCl_6]$ and $[P_{666,14}]_3[YCl_6]$.

Table 1 Er(III)/Y(III) mixed ILs 1–6

Item	IL 1	IL 2	IL 3	IL 4	IL 5	IL 6
Er(III)/mol %	0	20	40	60	80	100
Y(III)/mol %	100	80	60	40	20	0

normalization of the data. As shown in Fig. 6, the quality magnetic susceptibility of the mixed ILs increased linearly as the mole fraction of Er(III) increased. Similarly, the speed of the Er(III) drop accelerated with the same tendency, as the magnetic force that pulled the droplet toward the magnet became stronger. The magnetism of the so-called ILs was originated from the strong paramagnetic nature of Er(III) [44]. Therefore, a new method of quantifying magnetic material content by magnetic susceptibility can be concluded as the linearly relationship between the mole fraction and the quality magnetic susceptibility of Er(III). In this way, the amount of paramagnetic Er(III) in the mixed ionic liquid can be directly determined by measuring the mass susceptibility. It is superior to inductively coupled plasma (ICP) method at least in the two aspects of simpleness and low reagent consumption. The test precision can be consistent with that of ICP determination when there is no magnetism mature in the ionic liquid. It is also a new test method to determine the content of rare earth by magnetic susceptibility.

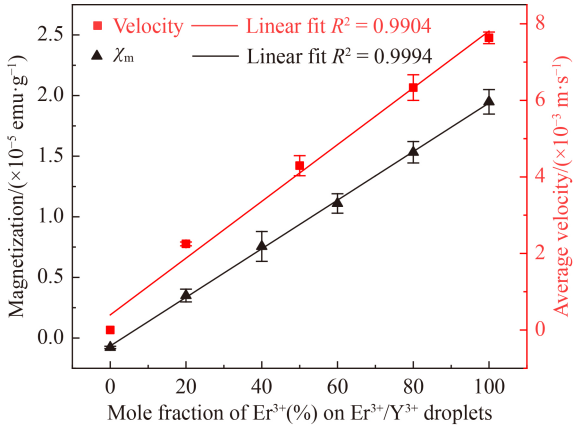

Fig. 6 Magnetization (black triangles) and average velocities (red squares) of the mixed ILs containing Er(III) and Y(III).

3.5 The proposed separation schematic plot

Magnetic separation has attracted increasing attention [45,46]. Based on the differences of ionic magnetic moment, rare-earth separation via QL strategy was proposed. However, the direct magnetic separation of inorganic salt was failure because of the large Brownian motion and the disordered state of RE(III) in the aqueous solution [15]. In this manuscript, ILs were introduced to improve the order degree of RE(III) dissolved in them and increase the magnetic susceptibility of paramagnetic RE(III), and then the difference between the paramagnetic RE(III) and diamagnetic RE(III) was enlarged. Therefore, the two RE(III) (group) were separated in the external magnetic field. As shown in Fig. 7, the experiments were conducted in the same apparatus where a magnet was placed on one side of the petri dish. No aggregation of diamagnetic ionic liquid would be observed, while an obvious magnetic migration phenomenon would be found near the magnet. As for the mixed paramagnetic and diamagnetic ILs, the paramagnetic RE(III) would be migrated and aggregated near the magnet and separated from the diamagnetic RE(III).

3.6 Magnetic separation of REEs in quasi-liquid system

To verify the assumption, a series of experiments were conducted in two aspects: (1) Magnetic induction experiments of pure ILs of Er(III), Ho(III) and Y(III). (2) Separation experiments of Er/Y, Ho/Y and Er/Ho mixed ILs in the petri dish (Fig. 7). Er(III) and Ho(III) dissolved in ILs are paramagnetic, which have no magnet in the absence of the external magnetic field because of the random directions of magnetic moments and the zero resultant force. In the presence of the external magnetic field, the paramagnetic Er(III) and Ho(III) in the ionic liquid will be arranged orderly and responded to the magnet, while the diamagnetic Y(III) will not be affected as there is no single electron in the electronic orbit.

3.6.1 Magnetic separation of Er(III)/Y(III) in quasi-liquid system

To express the magnetic induction phenomenon of $[P_{666,14}]_3[ErCl_6]$ and $[P_{666,14}]_3[YCl_6]$, the experiments

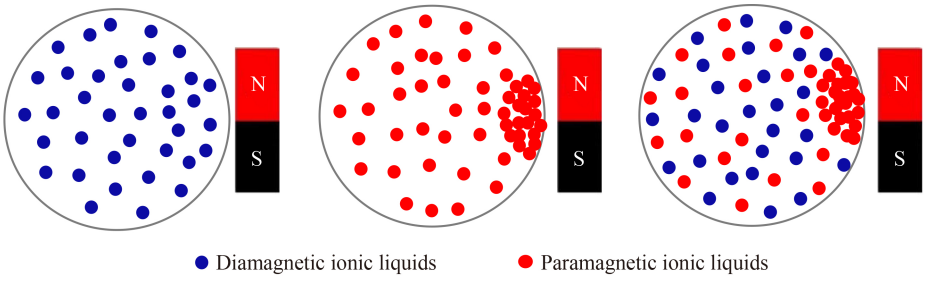

Fig. 7 Magnetic separation of REEs in the QL system diagram.

were performed carefully (Fig. 8). The magnetic field source was provided by a cuboid Nd–Fe–B magnet with the maximum surface magnetic field intensity of 3800 Oe (measured by a Gaussian meter). The QL system was constructed by dissolving $RECl_3$ in $[P_{666,14}][Cl]$. Then, each drop of 0.1 mL $[P_{666,14}]_3[ErCl_6]$ and $[P_{666,14}]_3[YCl_6]$ were set in the petri dish and their movement were investigated carefully in the magnetic field. To smoothen the surface, a small amount of water was added and it supported the ILs with lower density. As shown in Fig. 8(A), paramagnetic $[P_{666,14}]_3[ErCl_6]$ had an obvious magnetic induction phenomenon but the diamagnetic $[P_{666,14}]_3[YCl_6]$ was fixed in its primary place from 0 s to 12 s. The average velocity of $[P_{666,14}]_3[ErCl_6]$ increased with an accelerating trend as time went by (Fig. 8(B)). The intrinsic mechanism can be explained as: The magnetic field intensity enhanced as the drop mover to the magnet. Then the rising tendency of average velocity was formed, growing rapidly in the beginning and gradually tending to be stable as the resistance force to motion increased to the value of magnetic force. As for $[P_{666,14}]_3[YCl_6]$, the average velocity was kept at zero all the time in the whole range of the magnetic field. Additionally, a series of experiments named as a–d, presenting as different liquid drops (0.1 mL each drop) of $[P_{666,14}]_3[ErCl_6]$ and $[P_{666,14}]_3[YCl_6]$ of 1:1, 2:2, 4:4 and 8:8, respectively, were designed to describe the separation properties. As shown in Fig. 8(D), the ILs of Er(III) and Y(III) were separated from each other under a maximum surface magnetic field intensity of 4200 Oe. The two samples near and far from the magnet were collected for further analysis by ICP.

The results showed that more $[P_{666,14}]_3[ErCl_6]$ were enriched near the magnet in Fig. 8(E), although the specific proportions were different from a to d. Accordingly, more $[P_{666,14}]_3[YCl_6]$ stayed at the original location far from the magnet (Fig. 8(F)). In groups a and b, $[P_{666,14}]_3[ErCl_6]$ and $[P_{666,14}]_3[YCl_6]$ could be completely separated as the former attracted to the magnet and the later remained motionless. However, part of $[P_{666,14}]_3[YCl_6]$ was carried by the moving $[P_{666,14}]_3[ErCl_6]$ ILs when the liquid drops (group c and d) were increased. The main reason can be concluded as many $[P_{666,14}]_3[YCl_6]$ drops were hindered on the magnetic swimming route of $[P_{666,14}]_3[ErCl_6]$ and moved along with $[P_{666,14}]_3[ErCl_6]$ under the adhesive force. Herein, the maximum $\beta_{Er/Y}$ could reach at 9.0 with a higher theorical separation factor than that in the tradition by

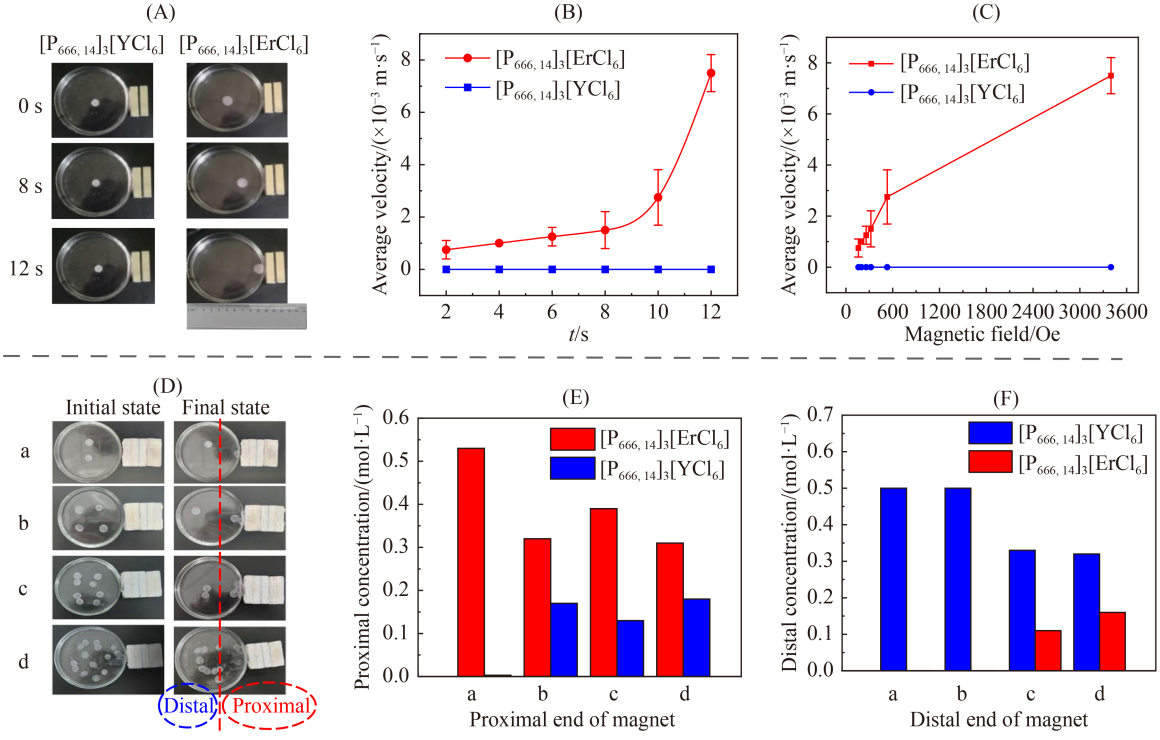

Fig. 8 Magnetic separation of Er(III)/Y(III) in QL system. (A) The magnetic induction phenomenon of $[P_{666,14}]_3[ErCl_6]$ and $[P_{666,14}]_3[YCl_6]$. (B) The average velocity of $[P_{666,14}]_3[ErCl_6]$ and $[P_{666,14}]_3[YCl_6]$ in different time. (C) The average velocity of $[P_{666,14}]_3[ErCl_6]$ and $[P_{666,14}]_3[YCl_6]$ in different magnetic fields (from the distal to the proximal end of the magnets). (D) Separations of different liquid drops (0.1 mL each drop) of $[P_{666,14}]_3[ErCl_6]$ and $[P_{666,14}]_3[YCl_6]$. a–d represent 1:1, 2:2, 4:4 and 8:8, respectively. The left graph: The initial state before magnetic movement, and the right graph: The final state when balance in motion is achieved. The two samples of each group were corrected for the proximal or distal end of the magnets and analysed for the concentration of $[P_{666,14}]_3[ErCl_6]$ and $[P_{666,14}]_3[YCl_6]$. (E) The concentrations of $[P_{666,14}]_3[ErCl_6]$ and $[P_{666,14}]_3[YCl_6]$ at the proximal end of the magnet in the a–d group. (F) The concentrations of $[P_{666,14}]_3[ErCl_6]$ and $[P_{666,14}]_3[YCl_6]$ at the distal end of the magnet in the a–d group.

P507 ($\beta_{Er/Y}$ = 1.4) [14]. The details of Er/Y mixed ionic liquid separation experiments were shown in Figs. S5–S6 in ESM. Finally, it was feasible to separate the Er(III) and Y(III) in the QL system based on their large magnetic moment difference.

3.6.2 Magnetic separation of Ho(III)/Y(III) in quasi-liquid system

Similarly, the magnetic separation of $[P_{666,14}]_3[HoCl_6]$ and $[P_{666,14}]_3[YCl_6]$ were conducted as shown in Fig. 9 under the same experimental conditions. The results showed that no movement of the diamagnetic $[P_{666,14}]_3[YCl_6]$ was observed as mentioned above, but an obvious magnetic induction phenomenon of the paramagnetic $[P_{666,14}]_3[HoCl_6]$ was similar to that of $[P_{666,14}]_3[ErCl_6]$ (Fig. 9(A)). Meanwhile, the influence tendency of movement time and the magnetic field on velocity was almost the same tendency as that of magnetic separation of Er(III)/Y(III) above. However, the separation efficiency of the two groups were different from each other. Considering the higher theoretical magnetic moment of Ho(III) (10.61 μ_B), its velocity was always larger than that of Er(III) (9.58 μ_B) at the same time or the magnetic field. For example, the average velocities of $[P_{666,14}]_3[HoCl_6]$ were 1.35×10^{-3} m·s^{-1} and 12.75×10^{-3} m·s^{-1} at the beginning 2 s and the whole process of 12 s, respectively. The results were 0.75×10^{-3} m·s^{-1} and 7.5×10^{-3} m·s^{-1} in the same situation of $[P_{666,14}]_3[ErCl_6]$ (Fig. 9(B)). The Ho(III) velocities were nearly 2 times higher than those of Er(III). It was consistent with the previous conclusion that the volume susceptibility of Ho(III) in the same state was greater than that of Er(III) (Fig. 2). As a result, the maximum $\beta_{Ho/Y}$ could be reached at 28.82, greater than that of $\beta_{Er/Y}$ with 9.0. It indicates that the bigger difference will result in the larger magnetic separation factor in the same situation.

Actually, $\beta_{Ho/Y}$ is approximately 1.64 by P507, while $\beta_{Er/Y}$ is only 1.4 [14]. The separation of Er/Y is also more difficult than that of Ho/Y based on the differences among Ho(III)(0.894 Å), Er(III)(0.881 Å) and Y(III) (0.880 Å) [15]. In a word, magnetic separation of Ho(III)/Y(III) in QL system is achieved at the magnetic field.

3.6.3 Magnetic separation of Er(III)/Ho(III) in quasi-liquid system

Based on the analysis above, magnetic separation of

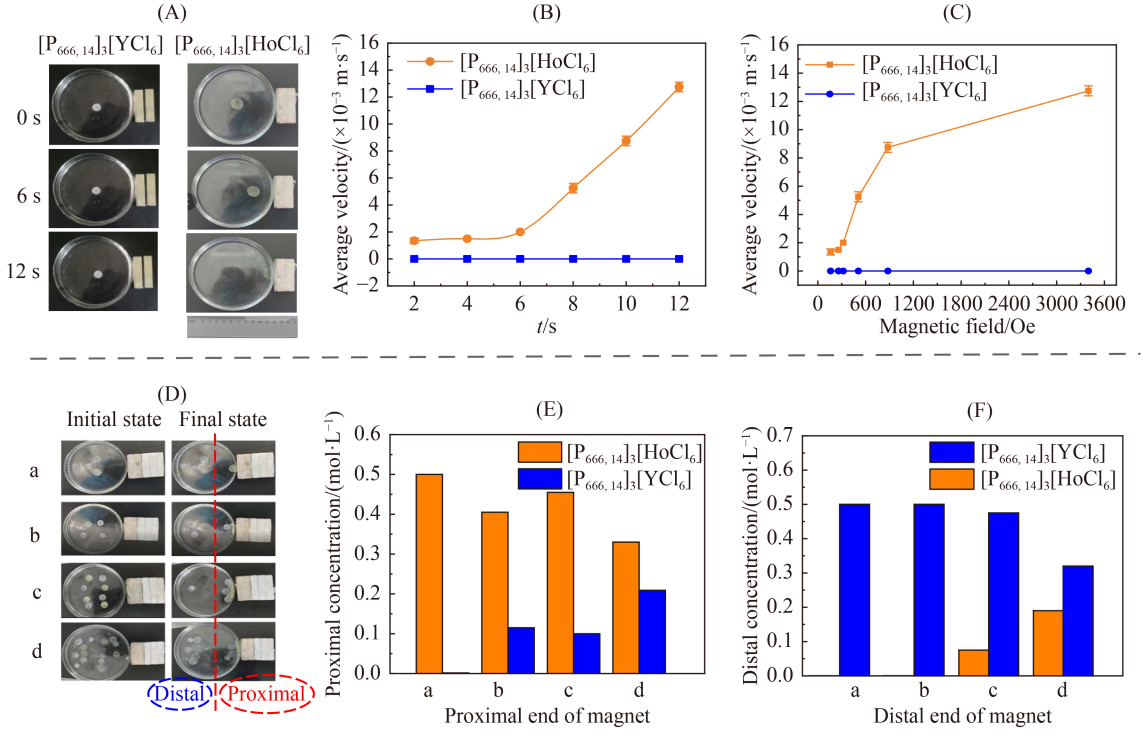

Fig. 9 Magnetic separation of Ho(III)/Y(III) in QL system. (A) The magnetic induction phenomenon of $[P_{666,14}]_3[HoCl_6]$ and $[P_{666,14}]_3[YCl_6]$. (B) The average velocity of $[P_{666,14}]_3[HoCl_6]$ and $[P_{666,14}]_3[YCl_6]$ in different time. (C) The average velocity of $[P_{666,14}]_3[HoCl_6]$ and $[P_{666,14}]_3[YCl_6]$ in different magnetic fields (from the distal to the proximal end of the magnets). (D) Separations of different liquid drops (0.1 mL each drop) of $[P_{666,14}]_3[HoCl_6]$ and $[P_{666,14}]_3[YCl_6]$. a–d represent 1:1, 2:2, 4:4 and 8:8, respectively. The left graph: The initial state before magnetic movement, and the right graph: The final state when balance in motion is achieved. The two samples of each group were corrected for the proximal or distal end of the magnets and analyzed for the concentration of $[P_{666,14}]_3[HoCl_6]$ and $[P_{666,14}]_3[YCl_6]$. (E) The concentrations of $[P_{666,14}]_3[HoCl_6]$ and $[P_{666,14}]_3[YCl_6]$ at the proximal end of the magnet in the a–d group. (F) The concentrations of $[P_{666,14}]_3[HoCl_6]$ and $[P_{666,14}]_3[YCl_6]$ at the distal end of the magnet in the a–d group.

Er(III)/Ho(III) in QL system was also tried in this manuscript. The experiments conditions were the same as section 3.6.1 and 3.6.2. As shown in Fig. 10, both $[P_{666,14}]_3[HoCl_6]$ and $[P_{666,14}]_3[ErCl_6]$ were attracted by the magnet although their average velocities were different from each other ($v_{Ho} > v_{Er}$). At the end of the magnetic separation experiments (12 s), the two REEs thoroughly moved to the magnet and almost no RE(III) could be detected in the group of a–d (Fig. 10(F)). It seemed that the magnetic separation of Er(III) and Ho(III) could not be achieved when equilibrium was reached. However, it might be possible to conduct separation in the kinetics perspective as shown in Fig. 10(B) and Fig. 10(C), due to the velocity differences of the two ILs in different time. More investigation should be conducted to separate these paramagnetic REEs with tiny differences of magnetic moments.

4 Conclusions

Based on the large differences of the magnetic moment among Ho(III), Er(III) and Y(III), rare earth magnetic separation with high efficiency has been achieved in QL system. The inoic liquid, as green solvent, has greatly enhanced the order of RE(III) and increased the differences between paramagnetic RE(III) and molecules diamagnetic RE(III). The volumetric magnetic susceptibility of $RECl_3 \cdot 6H_2O$ crystal, $[P_{666,14}]_3[RECl_6]$ and $RECl_3$ in aqueous solution are different from one another, although they have the same theoretical magnetic moment with the same RE(III). The volumetric magnetic susceptibility of the three states lies as: $RECl_3 \cdot 6H_2O(S)$ > $[P_{666,14}]_3[RECl_6](QL)$ > $RECl_3$ water solution(L) (RE presents as Er or Ho herein).

As a result, the paramagnetic $[P_{666,14}]_3[ErCl_6]$ and $[P_{666,14}]_3[HoCl_6]$ had obvious induction phenomena, aggregated near the magnet. However, the diamagnetic $[P_{666,14}]_3[YCl_6]$ had no induction phenomenon in the magnetic field. Then, a series of experiments were conducted to separate Er/Y, Ho/Y and Er/Ho in QL system. The results showed that the separation factors of Er/Y and Ho/Y were achieved at 9.0 and 28.82, respectively. They were obviously higher than those of the traditional separation method with $\beta_{Er/Y}$ and $\beta_{Ho/Y}$ of 1.4 and 1.64 by P507, which was based on the tiny ionic

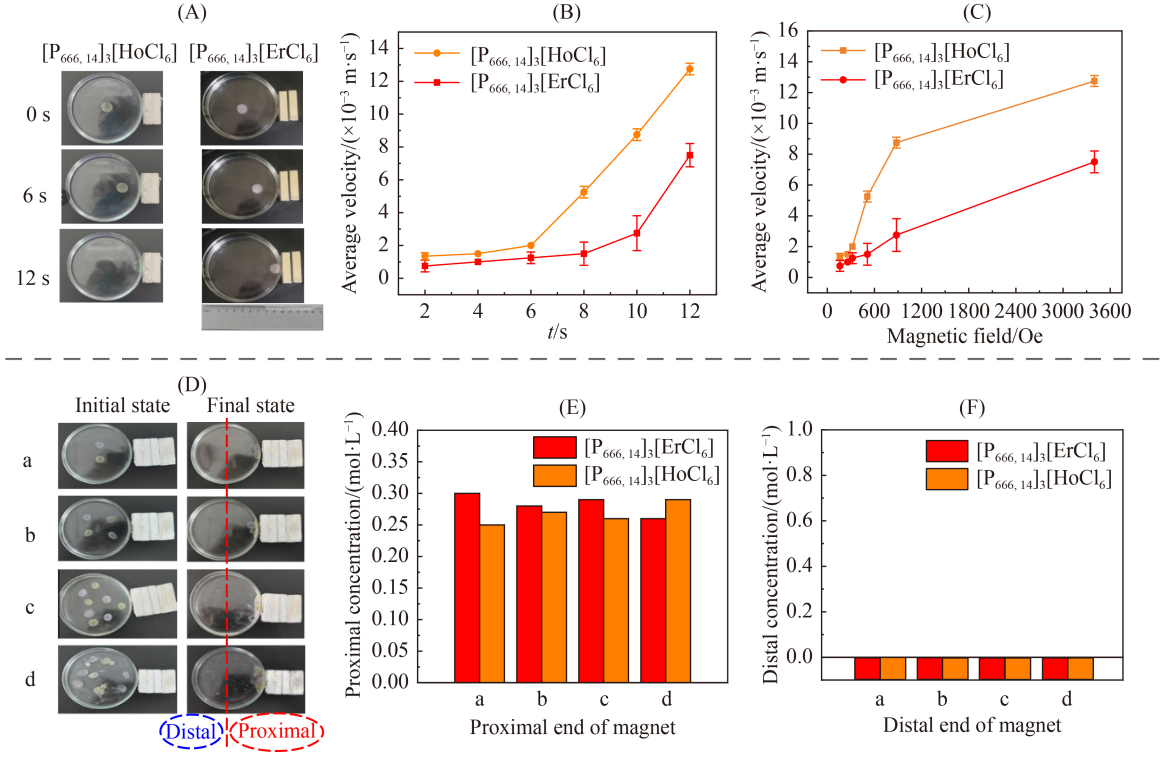

Fig. 10 Magnetic separation of Er(III)/Ho(III) in QL system. (A) The magnetic induction phenomenon of $[P_{666,14}]_3[ErCl_6]$ and $[P_{666,14}]_3[HoCl_6]$. (B) The average velocity of $[P_{666,14}]_3[ErCl_6]$ and $[P_{666,14}]_3[HoCl_6]$ in different time. (C) The average velocity of $[P_{666,14}]_3[ErCl_6]$ and $[P_{666,14}]_3[HoCl_6]$ in different magnetic fields (from the distal to the proximal end of the magnets). (D) Separations of different liquid drops (0.1 mL each drop) of $[P_{666,14}]_3[ErCl_6]$ and $[P_{666,14}]_3[HoCl_6]$. a–d represent 1:1, 2:2, 4:4 and 8:8, respectively. The left graph: The initial state before magnetic movement, and the right graph: The final state when balance in motion is achieved. The two samples of each group were corrected for the proximal or distal end of the magnets and analysed for the concentration of $[P_{666,14}]_3[ErCl_6]$ and $[P_{666,14}]_3[HoCl_6]$. (E) The concentrations of $[P_{666,14}]_3[ErCl_6]$ and $[P_{666,14}]_3[HoCl_6]$ at the proximal end of the magnet in the a–d group. (F) The concentrations of $[P_{666,14}]_3[ErCl_6]$ and $[P_{666,14}]_3[HoCl_6]$ at the distal end of the magnet in the a–d group.

radius difference. However, the separation of Er(III) and Ho(III) seemed difficult in the magnetic field due to their similar magnetism, but it might be possible in kinetics the perspective because of their velocity differences. To be concluded, it is with great potential to develop a green, efficient and sustainable magnetic separation process based on the differences of the RE(III) magnetic moment.

Furthermore, the separation efficiency may be increased via designing optimized magnetic rare earth ILs, introducing high magnetic fields and developing suitable process. The work provides a new perspective on green separation of rare earth elements.

Acknowledgments This research was supported by the National Natural Science Foundation of China (Grant No. 22008244), Rare Earth Industry Guidance Fund Project (Grant No. IAGM2020DB03), Self-Deployed Projects of Ganjiang Innovation Academy, Chinese Academy of Sciences (Grant No. E055A002), the Key Research Program of the Chinese Academy of Sciences (Grant No. ZDRW-CN-2021-3-2) and Special Research Assistant Project of the Chinese Academy of Sciences. Collaborative Innovation Center for Development and Utilization of Rare Metal Resources Co-sponsored by Ministry of Education and Jiangxi Province, Jiangxi University of Science and Technology (JXUST-XTCX-2022-01). The authors are grateful for the assistance from Professor Ling Wang of Analysis and Test Centre, Institute of Process Engineering, Chinese Academy of Sciences in MPMS-3 (Magnetic Property Measurement System).

Electronic Supplementary Material Supplementary material is available in the online version of this article at https://dx.doi.org/10.1007/s11705-022-2189-4 and is accessible for authorized users.

References

1. Eliseeva S V, Bünzli J C G. Rare earths: jewels for functional materials of the future. New Journal of Chemistry, 2011, 35(6): 1165–1176
2. Jiang Q, Cheng J Y, Gao Z Q. Direct synthesis of dimethyl carbonate over rare earth oxide supported catalyst. Frontiers of Chemical Engineering in China, 2007, 1(3): 300–303
3. Massari S, Ruberti M. Rare earth elements as critical raw materials: focus on international markets and future strategies. Resources Policy, 2013, 38(1): 36–43
4. Habashi F. Extractive metallurgy of rare earths. Canadian Metallurgical Quarterly, 2013, 52(3): 224–233
5. Xie F, Zhang T A, Dreisinger D, Doyle F. A critical review on solvent extraction of rare earths from aqueous solutions. Minerals Engineering, 2014, 56: 10–28
6. Rout A, Binnemans K. Liquid–liquid extraction of europium(III) and other trivalent rare-earth ions using a non-fluorinated functionalized ionic liquid. Dalton Transactions (Cambridge, England), 2014, 43(4): 1862–1872
7. Depuydt D, Dehaen W, Binnemans K. Solvent extraction of scandium(III) by an aqueous biphasic system with a nonfluorinated functionalized ionic liquid. Industrial & Engineering Chemistry Research, 2015, 54(36): 8988–8996
8. Li D Q. A review on yttrium solvent extraction chemistry and separation process. Journal of Rare Earths, 2017, 35(2): 107–119
9. Chen Y H, Wang H Y, Pei Y C, Wang J J. A green separation strategy for neodymium(III) from cobalt(II) and nickel(II) using an ionic liquid-based aqueous two-phase system. Talanta, 2018, 182: 450–455
10. Hérès X, Blet V, Di Natale P, Ouaattou A, Mazouz H, Dhiba D, Cuer F. Selective extraction of rare earth elements from phosphoric acid by ion exchange resins. Metals, 2018, 8(9): 682–698
11. Li F J, Wang Y L, Su X, Sun X Q. Towards zero-consumption of acid and alkali recycling rare earths from scraps: a precipitation-stripping-saponification extraction strategy using CYANEX®572. Journal of Cleaner Production, 2019, 228: 692–702
12. Li F J, Yan J J, Zhang X P, Wang N, Dong H F, Bai L, Gao H S. Removal of trace aluminum impurity for high-purity $GdCl_3$ preparation using an amine-group-functionalized ionic liquid. Industrial & Engineering Chemistry Research, 2021, 60(30): 11241–11250
13. Zhang J, Zhao B D, Schreiner B. Separation Hydrometallurgy of Rare Earth Elements. Heidelberg: Springer, 2016: 5–7
14. Wang X L, Li W, Meng S, Li D Q. The extraction of rare earths using mixtures of acidic phosphorus-based reagents or their thio-analogues. Journal of Chemical Technology and Biotechnology (Oxford, Oxfordshire), 2006, 81(5): 761–766
15. Moeller T. The Chemistry of the Lanthanides. Oxford: Pergamon Press, 1973: 6–9
16. Yang H J, Peng F, Schier D E, Markotic S A, Zhao X, Hong A N, Wang Y X, Feng P Y, Bu X H. Selective crystallization of rare-earth ions into cationic metal–organic frameworks for rare-earth separation. Angewandte Chemie International Edition, 2021, 60(20): 11148–11152
17. Noddack W, Noddack I, Wicht E. Separate the rare earths in the inhomogeneous magnetic field. Zeitschrift fur elektrochemie, 1958, 62(1): 77–85 (In German)
18. Higgins R F, Cheisson T, Cole B E, Manor B C, Carroll P J, Schelter E J. Magnetic field directed rare-earth separations. Angewandte Chemie International Edition, 2020, 59(5): 1851–1856
19. Yang X G, Tschulik K, Uhlemann M, Odenbach S, Eckert K. Enrichment of paramagnetic ions from homogeneous solutions in inhomogeneous magnetic fields. Journal of Physical Chemistry Letters, 2012, 3(23): 3559–3564
20. Faris N, Ram R, Tardio J, Bhargava S, Pownceby M I. Characterisation of a ferruginous rare earth bearing lateritic ore and implications for rare earth mineral processing. Minerals Engineering, 2019, 134: 23–36
21. Pearse G, Borduas J, Gervais T, Menard D, Seddaoui D, Ung B. Method and system for magnetic separation of rare earths. US Patent, 166788A1, 2014–06-19
22. Wang K Y, Adidharma H, Radosz M, Wan P Y, Xu X, Russell C K, Tian H J, Fan M H, Yu J. Recovery of rare earth elements with ionic liquids. Green Chemistry, 2017, 19(19): 4469–4493
23. Prodius D, Mudring A V. Rare earth metal-containing ionic liquids. Coordination Chemistry Reviews, 2018, 363: 1–16
24. Machida H, Taguchi R, Sato A, Florusse L J, Peters C J, Smith R L Jr. Measurement and correlation of supercritical CO_2 and ionic liquid systems for design of advanced unit operations. Frontiers of

Chemical Engineering in China, 2009, 3(1): 12–19
25. Greer A J, Jacquemin J, Hardacre C. Industrial applications of ionic liquids. Molecules, 2020, 25(21): 5207–5237
26. Zhang S N, Wang X Y, Yao J, Li H R. Electron paramagnetic resonance studies of the chelate-based ionic liquid in different solvents. Green Energy & Environment, 2020, 5(3): 341–346
27. Shamsuri A A, Abdan K, Jamil S N A M. Properties and applications of cellulose regenerated from cellulose/imidazolium-based ionic liquid/co-solvent solutions: a short review. e-Polymers, 2021, 21: 869–880
28. Hayashi S, Hamaguchi H O. Discovery of a magnetic ionic liquid [bmim]$FeCl_4$. Chemistry Letters, 2004, 33(12): 1590–1591
29. Hayashi S, Saha S, Hamaguchi H O. A new class of magnetic fluids: [bmim]$FeCl_4$ and n[bmim]$FeCl_4$ ionic liquids. IEEE Transactions on Magnetics, 2006, 42(1): 12–14
30. Dong K, Zhang S J, Wang Q. A new class of ion–ion interaction: Z-bond. Science China Chemistry, 2015, 58(3): 495–500
31. Zhang S J, Sun J, Zhang X C, Xin J Y, Miao Q Q, Wang J J. Ionic liquid-based green processes for energy production. Chemical Society Reviews, 2014, 43(22): 7838–7869
32. Zhang S J, Wang Y L, He H Y, Huo F, Lu Y M, Zhang X C, Dong K. A new era of precise liquid regulation: quasi-liquid. Green Energy & Environment, 2017, 2(4): 329–330
33. Wang Y L, He H Y, Wang C L, Lu Y, Dong K, Huo F, Zhang S J. Insights into ionic liquids: from Z-bonds to quasi-liquids. Journal of the American Chemical Society Au, 2022, 2(3): 543–561
34. Lu Y M, Chen W, Wang Y L, Huo F, Zhang L, He H, Zhang S J. A space-confined strategy toward large-area two-dimensional crystals of ionic liquid. Physical Chemistry Chemical Physics, 2020, 22(4): 1820–1825
35. Kubota F, Shigyo E, Yoshidai W, Goto M. Extraction and separation of Pt and Pd by an imidazolium-based ionic liquid combined with phosphonium chloride. Solvent Extraction Research and Development, Japan, 2017, 24(2): 97–104
36. Hughes I D, Dane M, Ernst A, Hergert W, Luders M, Poulter J, Staunton J B, Svane A, Szotek Z, Temmerman W M. Lanthanide contraction and magnetism in the heavy rare earth elements. Nature, 2007, 446(7136): 650–653
37. Li Y T, Li Y J, Yang Z X, Zhang X J, Zeng F M, Li C, Lin H, Su Z M, Mahadevan C K, Liu J H. The structure and liquid flow effect of melt during NaCl crystal growth. Crystal Research and Technology, 2020, 55(7): 1900229
38. Hayashi S, Ozawa R, Hamaguchi H O. Raman spectra, crystal polymorphism, and structure of a prototype ionic-liquid [bmim]Cl. Chemistry Letters, 2003, 32(6): 498–499
39. Katayanagi H, Hayashi S, Hamaguchi H O, Nishikawa K. Structure of an ionic liquid, 1-*n*-butyl-3-methylimidazolium iodide, studied by wide-angle X-ray scattering and raman spectroscopy. Chemical Physics Letters, 2004, 392(4): 460–464
40. Ozawa R, Hayashi S, Saha S, Kobayashi A, Hamaguchi H O. Rotational isomerism and structure of the 1-butyl-3-methylimidazolium cation in the ionic liquid state. Chemistry Letters, 2003, 32(10): 948–949
41. Saha S, Hayashi S, Kobayashi A, Hamaguchi H O. Crystal structure of 1-butyl-3-methylimidazolium chloride. A clue to the elucidation of the ionic liquid structure. Chemistry Letters, 2003, 32(8): 740–741
42. Habenschuss A, Spedding F H. The coordination (hydration) of rare earth ions in aqueous chloride solutions from X-ray diffraction. I. $TbCl_3$, $DyCl_3$, $ErCl_3$, $TmCl_3$, and $LuCl_3$. Journal of Chemical Physics, 1979, 70(6): 2797–2806
43. Starzak M, Mathlouthi M. Cluster composition of liquid water derived from laser-Raman spectra and molecular simulation data. Food Chemistry, 2003, 82(1): 3–22
44. Rodrigues I R, Lukina L, Dehaeck S, Colinet P, Binnemans K, Fransaer J. Magnetophoretic sprinting: a study on the magnetic properties of aqueous lanthanide solutions. Journal of Physical Chemistry C, 2018, 122(41): 23675–23682
45. Shirvani S, Mallah M H, Moosavian M A, Safdari J. Magnetic ionic liquid in magmolecular process for uranium removal. Chemical Engineering Research & Design, 2016, 109: 108–115
46. Trujillo-Rodriguez M J, Nacham O, Clark K D, Pino V, Anderson J L, Ayala J H, Afonso A M. Magnetic ionic liquids as non-conventional extraction solvents for the determination of polycyclic aromatic hydrocarbons. Analytica Chimica Acta, 2016, 934: 106–113